

A numerical model for density-and-viscosity-dependent flows in two-dimensional variably saturated porous media

Michel C. Boufadel ^{a,*}, Makram T. Suidan ^a, Albert D. Venosa ^b

^a *Department of Civil and Environmental Engineering, University of Cincinnati, Cincinnati, OH, USA*

^b *U.S. Environmental Protection Agency, National Risk Management Research Laboratory, Cincinnati, OH 45269, USA*

Received 29 June 1998; revised 20 November 1998; accepted 20 November 1998

Abstract

We present a formulation for water flow and solute transport in two-dimensional variably saturated media that accounts for the effects of the solute on water density and viscosity. The governing equations are cast in a dimensionless form that depends on six dimensionless groups of parameters. These equations are discretized in space using the Galerkin finite element formulation and integrated in time using the backward Euler scheme with mass lumping. The modified Picard method is used to linearize the water flow equation. The resulting numerical model, the MARUN model, is verified by comparison to published numerical results. It is then used to investigate beach hydraulics at seawater concentration (about 30 g l^{-1}) in the context of nutrients delivery for bioremediation of oil spills on beaches. Numerical simulations that we conducted in a rectangular section of a hypothetical beach revealed that buoyancy in the unsaturated zone is significant in soils that are fine textured, with low anisotropy ratio, and/or exhibiting low physical dispersion. In such situations, application of dissolved nutrients to a contaminated beach in a freshwater solution is superior to their application in a seawater solution. Concentration-engendered viscosity effects were negligible with respect to concentration-engendered density effects for the cases that we considered. © 1999 Elsevier Science B.V. All rights reserved.

Keywords: Beaches; Interface; Freshwater; Saltwater; Bioremediation

* Corresponding author. Environmental Engineering and Science Department, Clemson University, Clemson, SC 29634, USA. Tel.: +1-864-656-5574; fax: +1-864-656-0672; e-mail: mboufad@ces.clemson.edu

1. Introduction

In many environmentally important cases of subsurface flow and transport, water flow occurs in variably saturated media and its density and viscosity depend on solute concentration. In such flow problems, the governing equations of water flow and solute transport become highly nonlinear. The first nonlinearity is due to the nonlinear relation between soil moisture and both pressure head and hydraulic conductivity. The second nonlinearity arises due to the coupling between the water flow and the solute transport equations. The primary coupling arises in the equations through the hydraulic conductivity (due to viscosity variation) and the body force term (due to density variation) of the fluid flow equation and the advection terms of the solute transport equation. A second coupling enters the equations through velocity-dependent hydrodynamic dispersion. These flows are denoted here as density-and-viscosity-dependent flows in variably saturated media.

Examples of these flows are found in many natural systems. Ronen et al. (1996) presented data showing upward freshwater movement from a confined freshwater aquifer to the highly saline unsaturated zone of the Dead Sea coastal area. Another example is water flow in beaches in the presence of incoming (seaward) fresh groundwater flow (Wise et al., 1994).

In this paper, a new formulation for density-and-viscosity-dependent flows in two-dimensional variably saturated media is presented. It is cast in a dimensionless form and implemented in a finite element model, the MARUN model (for MARine UNSaturated). The MARUN model is verified by comparison to published numerical results and used in an illustrative example to investigate buoyancy effects in a rectangular section of a hypothetical variably saturated beach. The approach adopted in the illustrative example consists of quantifying the effects of capillarity, anisotropy, and mechanical dispersion on the spread of a freshwater plume in a saline two-dimensional variably saturated porous medium. The numerical results of the example provide guidelines for the selection of the best application strategy of dissolved nutrients to enhance the biodegradation of oil spills on beaches (Venosa et al., 1996; Wrenn et al., 1997; Boufadel et al., 1998a).

2. Previous modeling studies

We were not able to find in the literature a two-dimensional model that accounts for the simultaneous effects of density and viscosity on water flow in two-dimensional variably saturated media. Most numerical models have been developed to simulate seawater intrusion in aquifers (the salt concentration is about 30 g l^{-1}). In such situations, aquifers were either assumed to be confined (Frind, 1982) or unconfined with the flow across the water table modeled using the specific yield approach (Huyakorn et al., 1987; Galeati et al., 1992; Xue et al., 1995). Viscosity effects were shown to be negligible under saturated flow conditions because at typical groundwater velocities, concentration-engendered density effects are dominant (Galeati et al., 1992; Schincariol et al., 1997). Another set of numerical models were intended to model high salt concentrations (known also as brines). These models have been used to simulate water

flow above salt rock formations and salt domes (Voss and Souza, 1987; Herbert et al., 1988; Oldenburg and Pruess, 1995), which are under active consideration for the storage of radioactive wastes in several countries.

Few numerical models that simulate density-dependent and/or viscosity-dependent flows in variably saturated media are reported in the literature. Usseglio-Polatera et al. (1990) presented numerical solutions (using the finite difference method) for density-dependent flows in two-dimensional variably saturated beaches. Forkel and Celia (1992) reported density-and-viscosity-dependent finite element solutions for the movement of high salinity waters (about 300 g l^{-1}) in one-dimensional variably saturated media. Boufadel et al. (1997) provided a detailed finite element formulation and a numerical model for density-dependent flows in one-dimensional variably saturated media.

The numerical models presented by Usseglio-Polatera et al. (1990) and Boufadel et al. (1997) are limited in application to seawater salt concentrations, and do not account for the effects of salt concentration on water viscosity. Furthermore, detailed formulation and solution of the two-dimensional density-dependent flow and salt transport equations were not provided by Usseglio-Polatera et al. (1990). Although the numerical model of Forkel and Celia (1992) simulates viscosity dependence and high salt concentrations, it is one dimensional and thus, does not allow simulation of a wide range of natural systems. The numerical model of Boufadel et al. (1997) suffers from this limitation too.

3. Model formulation

The dependence of water density on the salt concentration (taken as sodium chloride, NaCl) can be obtained by fitting a regression curve for the density versus salt concentration (p. D261 of CRC Handbook of Chemistry and Physics, 1982–1983):

$$\frac{\rho^*}{\rho_o^*} = (1.0 + \epsilon^* c^*) = \beta \quad (1)$$

where $(^*)$ represents dimensional quantities, $\rho_o^* = 0.9982 \text{ kg l}^{-1}$ is the freshwater density at 20°C , c^* is the sodium chloride concentration expressed in grams of salt/liter of solution, ϵ^* is estimated at $6.46 \times 10^{-4} \text{ l g}^{-1}$ with a coefficient of determination $r^2 = 0.9994$. Similarly, the dynamic viscosity μ^* can be related to the salt concentration by the empirical relation fitted to the data from p. D261 of CRC Handbook of Chemistry and Physics (1982–1983):

$$\frac{\mu_o^*}{\mu^*} = (1.0 - \xi^* c^*) = \delta \quad (2)$$

where $\mu_o^* = 0.001 \text{ kg m}^{-1} \text{ s}^{-1}$ is the freshwater dynamic viscosity and $\xi^* = 1.566 \times 10^{-3} \text{ l g}^{-1}$ with a coefficient of determination $r^2 = 0.9989$.

In the absence of source/sink terms, the equation for the conservation of the fluid mass (water + salt) is (Huyakorn and Pinder, 1983; Boufadel, 1998):

$$\frac{\partial(\beta\phi S)}{\partial t^*} = \frac{\partial\left(\beta\delta K_x^* \frac{\partial\psi^*}{\partial x^*}\right)}{\partial x^*} + \frac{\partial\left(\beta\delta K_z^* \frac{\partial\psi^*}{\partial z^*}\right)}{\partial z^*} + \frac{\partial(\beta^2\delta K_z^*)}{\partial z^*} \quad (3)$$

where $\phi [-]$ is the porosity of the medium (where $[-]$ = dimensionless) and $S [-]$ is the water saturation ratio of soil moisture with a value of 1 implying fully saturated soil, $\psi^* = P^*/(\rho_o^* g^*) [L]$ is the pressure head and K_x^* and K_z^* are the horizontal and vertical hydraulic freshwater hydraulic conductivities $[L T^{-1}]$ given by $K_x^* = k_x^* \rho_o^* g/\mu_o^*$ and $K_z^* = k_z^* \rho_o^* g/\mu_o^*$, respectively, and k_x^* and k_z^* are the horizontal and vertical hydraulic permeabilities.

The soil moisture and the freshwater hydraulic conductivity are correlated by the model of van Genuchten (1980):

$$\text{for } \psi^* \geq 0.0, \quad S = 1.0, \quad K_x^* = K_{x_o}, \quad \text{and} \quad K_z^* = K_{z_o} \quad (4a)$$

where K_{x_o} and K_{z_o} are the saturated horizontal and vertical hydraulic conductivities, respectively. For $\psi^* \leq 0.0$, the effective saturation ratio, S_e , is given by:

$$S_e = \frac{S - S_r}{1 - S_r} = \left[\frac{1}{1 + (\alpha^* |\psi^*|)^n} \right]^m \quad (4b)$$

and K_x^* and K_z^* are given by:

$$K_i^* = K_{i_o} S_e^{1/2} \left[1 - (1 - S_e^{1/m})^m \right]^2 \quad (4c)$$

where $j = x, z$; $m = 1 - (1/n)$, S_r is the residual saturation ratio, and $|\psi^*|$ is the absolute value of ψ^* . The parameter α^* represents a characteristic pore size and higher α^* values imply a coarser material. The inverse of α^* provides an estimate of the capillary fringe. The term n represents the uniformity of the pores and higher values of n imply a more uniform pore-size distribution (van Genuchten, 1980; Boufadel et al., 1998b).

In the absence of concentration source/sink term, the conservation of solute equation is expressed as (Gureghian, 1983; Huyakorn and Pinder, 1983, p. 209):

$$\frac{\partial(\phi S c^*)}{\partial t^*} = \nabla(\phi S \underline{D}^* \nabla \cdot c^*) - \nabla(\underline{q}^* c^*) \quad (5)$$

where \underline{D}^* is the physical dispersion tensor (it includes mechanical dispersion and diffusion) and \underline{q}^* is the Darcy flux vector. Eqs. (3) and (5) are rearranged (see Appendix A) to give the flow equation in the form:

$$\beta\phi \frac{\partial S}{\partial t^*} + \beta S_o^* S \frac{\partial \psi^*}{\partial t^*} + \phi S \frac{\partial \beta}{\partial t^*} = \frac{\partial \left(\beta \delta K_x^* \frac{\partial \psi^*}{\partial x^*} \right)}{\partial x^*} + \frac{\partial \left(\beta \delta K_z^* \frac{\partial \psi^*}{\partial z^*} \right)}{\partial z^*} + \frac{\partial \left(\beta^2 \delta K_z^* \right)}{\partial z^*} \quad (6)$$

where $S_o^* [L^{-1}]$ is the coefficient of storage per unit fluid weight. The salt transport equation is rewritten in the form:

$$\phi S \frac{\partial c^*}{\partial t^*} = \beta \nabla(\phi S \underline{D}^* \nabla c^*) - \underline{q}^* \nabla c^* \quad (7)$$

The presence of β in the first term of the right-hand side of Eq. (7) results in an increase in physical dispersion. Although the increase is small at low salt concentration ($\beta = 1.03$), it can alter greatly the hydrodynamics at high salt concentrations ($\beta = 1.2$).

4. Non-dimensionalization

Although model results presented in dimensional form are easy to interpret, they do not succeed generally in illustrating the interactions of major physical phenomena. A dimensionless formulation of the governing equations obtained in Section 3 is presented.

Let $x = x^*/L_z$, $z = z^*/L_z$, $S_o = S_o^*/L_z$, $\psi = \psi^*/L_z$, $\underline{D} = \underline{D}^*/(L_z K_{z_o})$, and $\alpha = \alpha^*/L_z$ where L_z is a characteristic length in the z direction (here taken as the height of the porous domain). In addition let $T_o = L_z/K_{z_o}$ be a characteristic time; T_o is the time needed for a water particle to cross the vertical distance L_z if the particle were moving at the constant speed K_{z_o} . Eq. (6) is rewritten in a dimensionless form:

$$\beta\phi \frac{\partial S}{\partial t} + \beta S_o S \frac{\partial \psi}{\partial t} + \phi S \frac{\partial \beta}{\partial t} = R \frac{\partial \left(\beta \delta K \frac{\partial \psi}{\partial x} \right)}{\partial x} + \frac{\partial \left(\beta \delta K \frac{\partial \psi}{\partial z} \right)}{\partial z} + \frac{\partial (\beta^2 \delta K)}{\partial z} \quad (8)$$

where R is the anisotropy ratio, K_{x_o}/K_{z_o} . Eq. (7) is written as:

$$S = 1.0, \quad K = 1.0, \quad \text{when } \psi \geq 0.0 \quad (9a)$$

when $\psi < 0.0$, S_e is given by:

$$S_e = \frac{S - S_r}{1 - S_r} = \left[\frac{1}{1 + (\alpha|\psi|)^n} \right]^m \quad (9b)$$

and K is given by:

$$K = S_e^{1/2} \left[1 - (1 - S_e^{1/m})^m \right]^2 \quad (9c)$$

The salt transport (Eq. (7)) is rewritten as:

$$\phi S \frac{\partial c^*}{\partial t} = \beta \nabla (\phi S \underline{D} \nabla c^*) - \underline{q} \nabla c^* \quad (10)$$

Although the concentration is reported in a dimensional form in Eq. (10), it could be very easily transformed to a dimensionless form by dividing by a reference concentration. This is not necessary, however, because Eqs. (1) and (2) provide density and viscosity effects in a dimensionless form. The dimensionless dispersion coefficients are given by:

$$\phi S D_{x_x} = a_L \frac{(q_x)^2}{\|q\|} + a_T \frac{(q_z)^2}{\|q\|} + \phi S \tau D_f \quad (11a)$$

$$\phi S D_{z_z} = a_T \frac{(q_x)^2}{\|q\|} + a_L \frac{(q_z)^2}{\|q\|} + \phi S \tau D_f \quad (11b)$$

$$\phi S D_{x_z} = \phi S D_{z_x} = (a_L - a_T) \frac{q_x q_z}{\|q\|} \quad (11c)$$

where $a_L = a_L^* / L_z$, $a_T = a_T^* / L_z$ are the dimensionless longitudinal and transverse dispersivities, respectively, and $D_f = D_f^* / (L_z K_{zo})$ is the dimensionless diffusion coefficient. The terms a_L^* and a_T^* are the dimensional dispersivities, $D_f^* [L^2 T^{-1}]$ is the dimensional diffusion coefficient, and $\tau [-]$ is the domain tortuosity.

Six dimensionless parameters emerge from the dimensionless formulation in Eqs. (8), (9a), (9b), (9c), (10), (11a), (11b) and (11c); they are R , n , α , a_L , a_T , and D_f . The parameter α can be seen as the ratio of the gravity forces (represented by L_z) to capillarity forces (represented by the inverse of α^*). It can be interpreted also as the ratio of the domain height to the height of the capillary fringe. The parameter D_f is the ratio of diffusion to a domain-based value of advection. The inverse of D_f can be interpreted as a domain-based Peclet number.

4.1. Advantages of the dimensionless formulation

A major advantage of the dimensionless formulation is that it provides guidelines for designing laboratory experiments dealing with solute transport in variably saturated media. The use of a porous medium in the laboratory setup presents an advantage over a Hele–Shaw cell (e.g., Wooding et al., 1997a,b) which cannot account for capillarity effects. The dimensionless formulation shows that the conservation of the values of the six dimensionless parameters is a necessary and sufficient condition to obtain the same hydraulics and hydrodynamics in two different systems.

An illustration of the applicability of the dimensionless formulation in designing laboratory experiments is given as follows: Suppose it is desired to use a laboratory setup to simulate water flow in a natural system $150 \text{ m} \times 600 \text{ m}$ (150 m is vertical). The dimensionless formulation shows that the geometry of the natural domain and the ratio of anisotropy need to be conserved. Boufadel (1998) showed that these restrictions can be removed if either the flow is uniform, physical dispersion is negligible with respect to advection, or if the dispersion coefficients can be approximated by constant quantities. Frind (1982) provided a thorough discussion on approximating velocity-dependent dispersion coefficients by constant dispersion coefficients.

Considering the general case for dispersion, suppose that a $6.0 \text{ m} \times 24.0 \text{ m}$ laboratory setup was selected (hence a 25-fold scale down). Suppose furthermore that the capillary fringe in the natural system is 1.0 m, which gives a value of $\alpha^* = 1.0 \text{ m}^{-1}$ in the natural system. The dimensionless formulation shows that correct scaling of the water flow requires $\alpha = L_z \alpha^*$ to be the same in the natural system and the laboratory setup, which results in $\alpha^* = 25 \text{ m}^{-1}$ in the laboratory setup. Hence, the value of the capillary fringe in the laboratory setup is 0.04 m, which can be easily achieved using a sand that is coarser than the one in the natural system. The saturated hydraulic conductivity of the laboratory sand is then measured and used in T_0 to transform the real (dimensional) time to a dimensionless time. Further discussion on the dimensionless formulation is provided elsewhere (Boufadel, 1998; Boufadel et al., 1998b).

A second advantage of the dimensionless formulation is that it provides a basis for comparison between various dimensional numerical solutions. This advantage was illustrated in Boufadel (1998) in dealing with the problem of Elder (1967), which is a high salinity scenario.

5. Model implementation

Eqs. (1), (2), (8), (9a), (9b), (9c) and (10) present a highly nonlinear system. In the case where the effect of salt on water density and viscosity is neglected ($\beta = 1$, $\delta = 1$) and $\psi < 0$, nonlinearity results from Eqs. (9b) and (9c). For $\psi \geq 0.0$, nonlinearity resides in the variation of c^* which affects the values of β and δ in both Eqs. (8) and (10). Hence, when these equations are solved numerically, the following approach is used: At the beginning of time step n , the concentrations are assumed known, the β and δ terms become inputs to the flow equation, and the modified Picard method (Celia et al., 1990) is used to obtain a solution for pressure heads. The Darcy fluxes are then computed and introduced into the transport equation (10), which is linearized by taking β as given from the previous time step or global coupling iteration. The concentrations of salt are then obtained and the β 's and the δ 's are then computed from Eqs. (1) and (2), respectively. For coupled solutions, the new values of β and δ are input to the flow equation at the beginning of the same time step n , and the procedure is repeated until pressure heads and concentration obtained at the end of the time step n cease to vary (within certain precision). For partially coupled solutions, the β and the δ values from time step $n - 1$ become the input to the flow and transport equations at time n . The updated values of soil moisture ratio S and the Darcy's fluxes from the flow equation are introduced along with the same values of β and δ to the transport equation which is then solved once. The updated values of β and δ are then entered to the flow equation at the beginning of the following time step $n + 1$, which is a mere updating. For uncoupled solution, β and δ are set at the value of 1.0. Thus in general, there can be two iterative loops: one loop for the flow equation (8) and one global loop to couple the flow and the transport equations through (1) and (2). The Darcy fluxes are computed using the finite element method (Yeh, 1981) because it ensures continuity of the Darcy flux across element boundaries.

The equations are discretized in space by the standard Galerkin method using triangular elements (Huyakorn and Pinder, 1983) and integrated in time using backward Euler with mass lumping (Celia et al., 1990). The empirical adaptive underrelaxation scheme developed by Cooley (1983) is adopted to alleviate nonlinearities in the flow equation. The linear systems are solved by the standard banded LU decomposition (Najem, 1982; Istok, 1989). More details on the MARUN model implementation are provided in Boufadel (1998).

6. Model verification

We were not able to find in the literature a well documented example for density-dependent flow in two-dimensional variably saturated media; Usseglio-Polatera et al. (1990) did not provide the parameters values used in their example. For this reason, the ability of the MARUN model to simulate the combined physical phenomena of density dependence and capillarity is verified by testing the MARUN model ability to simulate these phenomena separately.

The first example, Example 1, illustrates the ability of the MARUN model to simulate density-dependent flows under saturated flow conditions in two-dimensional

media. Example 2 illustrates the ability of the MARUN model to simulate solute transport in unsaturated two-dimensional media without density or viscosity dependence. The ability of the MARUN model to simulate density-and-viscosity-dependent flows in variably saturated one-dimensional media was verified in an unpublished work by comparison to Example 3 of Forkel and Celia (1992). The water flow component of the MARUN model was verified in the work by Boufadel et al. (1998b). The ability of the MARUN model to simulate highly saline (300 g l^{-1}) density-dependent flows in two-dimensional saturated media was tested in the work by Boufadel (1998).

The dimensionless formulation is not used in Examples 1 and 2 for brevity.

6.1. Example 1: Seawater intrusion in a confined aquifer

This example concerns groundwater flow and salt transport in a coastal confined aquifer. The problem considered is known as the seawater intrusion problem of Henry (1964) and is described schematically in Fig. 1. As depicted in Fig. 1, freshwater enters the aquifer on the right face, and the coastal side corresponds to the left face. Boundary conditions used in our numerical simulation are also shown. The aquifer region was represented by a grid $N_x \times N_z = 21 \times 11$ forming 231 nodes and 400 right angle triangles. The orientation of the diagonals was the same throughout the mesh. The time step Δt was allowed to increase gradually by a factor of 1.2 from 0.2 to 10 min. Fig. 2a and b compare the MARUN model numerical results with 0.5 isochlor computed by Frind (1982) at steady state under the assumption of a constant dispersion coefficient $\tau \phi D_f^* = 6.6 \times 10^{-6} \text{ m}^2 \text{ s}^{-1}$ and velocity-dependent dispersion ($a_L^* = a_T^* = 0.035 \text{ m}$), respectively.

The results obtained from partial coupling were indistinguishable from the ones obtained with full coupling. Thus, only the partial coupling solution is compared to the results of Frind (1982) in Fig. 2a and b, where the agreement is very good. The 0.1 and 0.9 isochlors are also shown for illustrative purposes. No apparent change in the solution

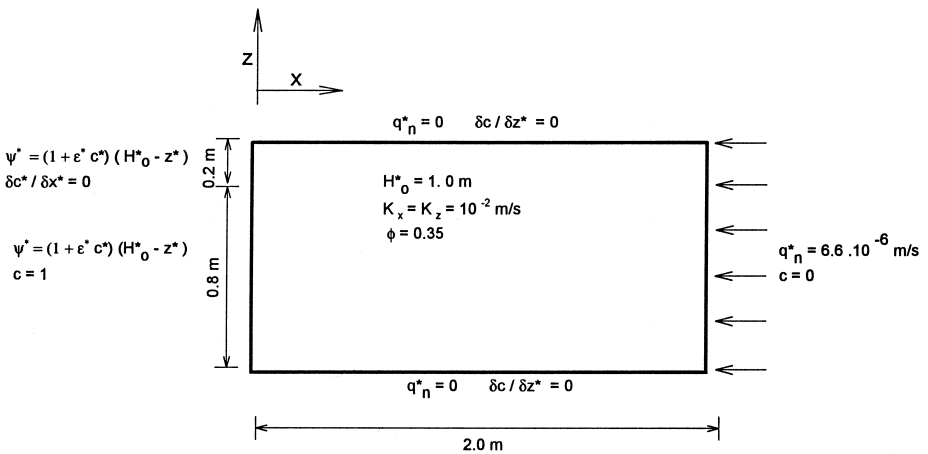


Fig. 1. Definition of Henry's problem and boundary conditions as simulated by Frind (1982).

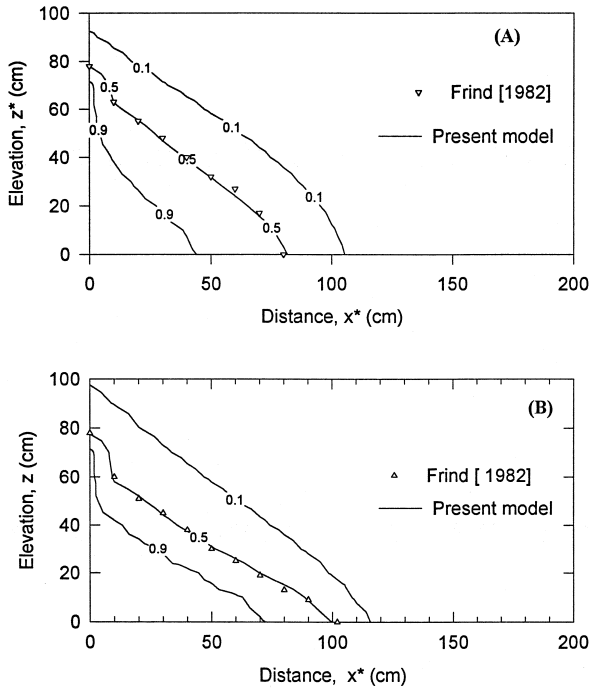


Fig. 2. Position of the isochlors at equilibrium (A) using constant dispersion coefficient and (B) using velocity dependent dispersion coefficients. The isochlors are reported as ratio of the maximum concentration of 38.7 g/l.

was observed when β was set equal to 1.0 in the transport equation (10). The solution was practically unchanged when the effects of salt concentration on water viscosity were accounted for, which supports the assumption that concentration-engendered viscosity effects are negligible in seawater intrusion problems.

The reader is referred to Croucher and O’Sullivan (1995) for a thorough numerical investigation on numerical solutions of Henry’s problem.

6.2. Example 2: Transport of a nonconservative solute in unsaturated media with no density dependence

This example is taken from Huyakorn et al. (1985) and concerns transport of a nonconservative solute in a rectangular cross section of an unsaturated soil with no density or viscosity dependence. Fig. 3 shows the domain geometry and the initial and boundary conditions. The temporal term in Eq. (7) is changed to:

$$\phi SR_d \left(\frac{\partial c^*}{\partial t^*} + \lambda^* c^* \right) \tag{12}$$

where λ^* represents the decay constant and R_d the retardation coefficient. Although λ^* is physically meaningless for salt transport (as salts do not decay), the retardation

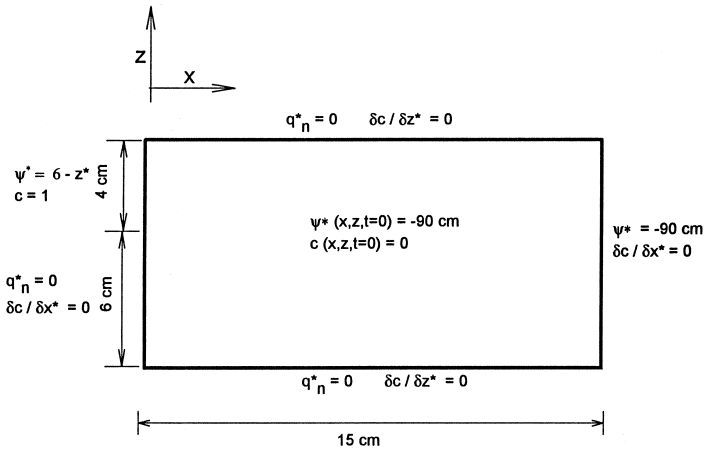


Fig. 3. Two-dimensional transport in an unsaturated slab (Huyakorn et al., 1985).

coefficient plays an important role in the transport of salts in colloidal-sized media (p. 127 of Freeze and Cherry, 1979). Nevertheless, the comparison is done here for numerical purposes. The terms β and δ were set to 1.0 in both the flow and transport equation, and the following empirical equations given by Huyakorn et al. (1985) were used to relate the saturation ratio and the hydraulic conductivity to pressure head:

$$S = 1 - (1 - S_r) \frac{\psi^*}{\psi_r^*} \tag{13a}$$

and

$$K_x^* = K_z^* = K_o \frac{S - S_r}{1 - S_r} \tag{13b}$$

with the values of S_r , ψ_r , and K_o given in Table 1 along with the other needed parameters. The domain was represented by a grid of 176 nodes and 300 triangular elements. The nodal spacing was $\Delta x = \Delta z = 1$ cm. Time increment values were

Table 1
Values of physical parameters used in Example 2

Parameter	Assigned value and unit
K_o	1 cm d ⁻¹
ϕ	0.45 [-]
$\Psi^*(x, z, 0)$	-90 cm
S_r	0.333 [-]
Ψ_r^*	-100 cm
$c(x, z, 0)$	0 [-]
a_L^*	1 cm
a_T^*	0 cm
τD_f^*	0.01 cm ² d ⁻¹
λ^*	0.001 d ⁻¹
R	2 [-]

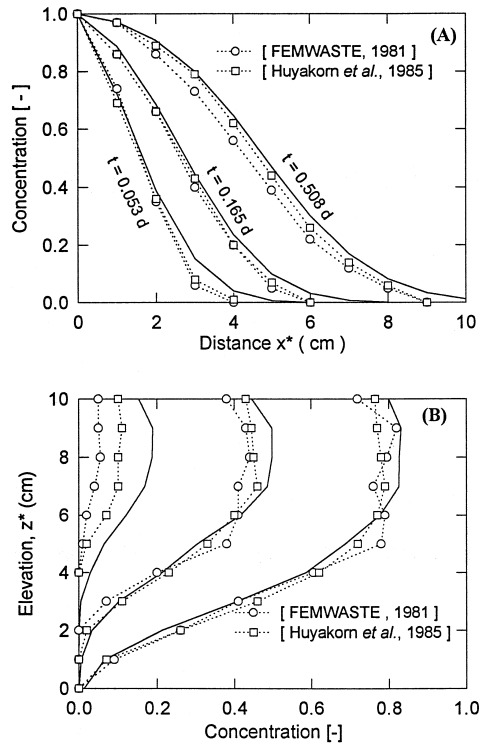


Fig. 4. (A) Computed horizontal distribution of solute concentration at $z = 10$ cm. (B) Computed vertical distribution of solute concentration at $x = 3$ cm. The present model results are the solid lines.

generated within the MARUN code using the algorithm: $\Delta t_1 = 0.01$ day, $\Delta t_k = 1.2$, $\Delta t_{k-1} \leq 0.05$ day. The transport simulation was performed for 15 time steps. The solutions obtained using the MARUN model are compared in Fig. 4 with the corresponding solutions obtained from the model of Huyakorn et al. (1985) and FEMWASTE (Yeh and Ward, 1981), as reported by Huyakorn et al. (1985). Evidently, the overall agreement of the MARUN model with the two numerical solutions is very good. The concentration distributions depicted in Fig. 4 are all smooth unlike FEMWASTE results. Although the profile predicted by the present model at time $t = 0.053$ day (Fig. 4b) is ahead of both models, the agreement at later times is very good. The relatively small smearing from the present model in the lower part of Fig. 4a resulted probably from the use of the fully implicit Euler scheme in the transport equation (7), whereas the two other codes used the Crank–Nicholson scheme, which is known to produce little numerical smearing (Pinder and Gray, 1977; Anderson et al., 1984).

7. Application

This application is designed to investigate the buoyancy of a freshwater plume in a beach containing seawater salt concentration of 30 g l^{-1} . The usefulness of this

example, Example 3, can be found in the practice of bioremediation of oil spills on beaches. Venosa et al. (1996) found that addition of dissolved nutrients to an oil-contaminated beach enhances oil biodegradation. They reported that a nutrient-nitrogen concentration of 2 mg l^{-1} achieves maximal oil biodegradation. The effectiveness of the bioremediation depends on contact between the added nutrients and the oil-polluted zone, which is less than about 25 cm below the beach surface (Gundlach, 1987). Ideally, nutrient concentrations in contact with the oil should be sufficient to support maximal growth rate of the oil-degrading bacteria, and this concentration must be maintained for the longest possible time. Therefore, maximizing the residence time of the nutrients in the contaminated zone of the beach is an important bioremediation goal.

Various application strategy of dissolved nutrients have been proposed. Wrenn et al. (1997) ran a tracer study on a Delaware beach subjected to tides and waves. They applied a solution of lithium nitrate on the beach surface at low tide to simulate nutrients application and they monitored lithium as a conservative tracer (i.e., it does not degrade or adsorb to the beach material). They observed a washout of the tracer from the beach within one tidal cycle. Wise et al. (1994) modeled the hydraulics and hydrodynamics of an alaskan beach subjected to freshwater inflow and tide. Based on their numerical results, they proposed to apply the nutrients in a trench landward of the beach and rely on the freshwater to carry it to the contamination zone at beach surface. The numerical model that they used was limited to the saturated zone of the beach, which results in a nutrients application strategy that underestimates the biodegradation of oil in the beach. This is because the contaminated zone, being near the beach surface, is under unsaturated flow conditions for long periods. If sufficient moisture exists in the contaminated zone to support a medium for microbial growth, biodegradation under unsaturated flow conditions is expected to occur at a higher rate than under saturated flow conditions. This is because the molar concentration of oxygen in air is about 10 times the maximum molar concentration of oxygen in water (which is dictated by the solubility limit of oxygen in water $\approx 8 \text{ mg l}^{-1}$). Therefore, a successful nutrients application strategy is one that provides nutrients to the unsaturated zone of the beach and maximizes their contact time with oil.

We investigate here the strategy of applying dissolved nutrients in a freshwater solution in a trench of a beach containing a uniform salt concentration. The trench is assumed to be located landward of the contaminated zone. This method of nutrients application is economically feasible if, for example, a freshwater pond is in proximity of the beach, such as in the case of the Kittiwake beach in Alaska (Wise et al., 1994). To quantify buoyancy effects, a comparison is made between the density-dependent results and the results obtained by assuming that the salt concentration does not engender density gradients (the salt acts thus as a tracer). For a beach containing a uniform seawater concentration, the ‘tracer’ case is the equivalent of adding the nutrients in a seawater solution (at the same salt concentration of the beach) to the trench. This is because the concentration of applied nutrients is usually too small to affect water density.

The effects of the beach hydraulic and hydrodynamic properties on the spreading of the water plume is studied. Specifically, the effects of α , R , and physical dispersion as the important influencing parameters are considered. Anisotropy in beaches can result

from alternating microscopic layers of fine and coarse sands (Waddell, 1976). Geological surveys on beaches revealed that there is no preferential direction for the layers; they could be horizontal, at a landward dip, or at seaward dip (Hayes, 1972). Therefore, it is assumed for the sake of simplicity that the principal directions of anisotropy coincide with the x and z axes (i.e., no dip). The domain under study is a rectangular section of hypothetical beach. The initial and boundary conditions are given in Fig. 5. Throughout this example we set $D_f = 0.0$, $\phi = 0.33$, $n = 2.0$, $S_r = 0.06$, and $\Delta t = 0.01$. An illustration of the salinity distribution at $t = 10$ is shown in Fig. 6 for $\alpha = 2.0$ and $R = 1.0$, and $a_L = a_T = 0.005$. The freshwater plume of the density-dependent case (Fig. 6b) spreads more in the unsaturated zone than that of the tracer case (Fig. 6a). The effects of a change in the capillary forces and/or anisotropy on the spread of the freshwater plume are investigated in Section 7.1.

7.1. Effect of capillarity and anisotropy

The MARUN model was run for various values of α and R while fixing the values of the remaining parameters. The effect of buoyancy is quantified using two criteria. The first criterion, criterion Z_m , is an area-based criterion. It represents the freshwater distribution in the saturated and the unsaturated zones of the domain. It is given as follows:

$$Z_m(\alpha, R) = \frac{\left(\frac{M_u}{M_s}\right)_{DD}}{\left(\frac{M_u}{M_s}\right)_T} \tag{14}$$

where M_i ($i = u, s$) represents the diluted water mass (i.e., for c strictly smaller than 30 g l^{-1}); the index u represents the unsaturated zone and the index s represents the saturated

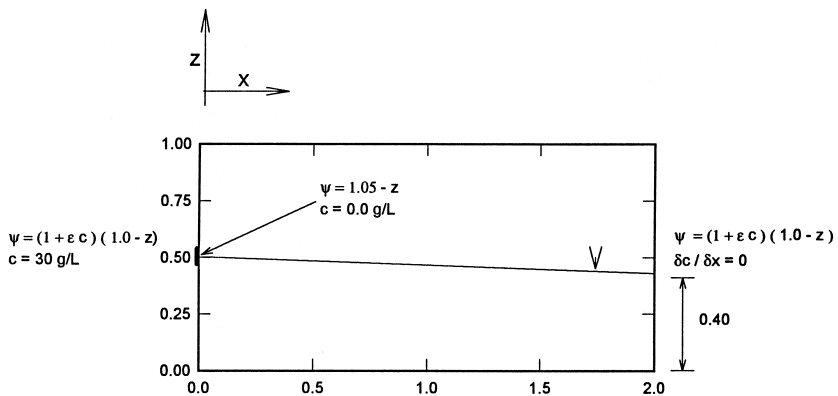


Fig. 5. Domain and boundary conditions for Example 3. The Dirichlet boundary conditions $\psi = 1.05 - z$ and $c = 0.0 \text{ g/l}$ are imposed at the elevations 0.48, 0.50, and 0.52.

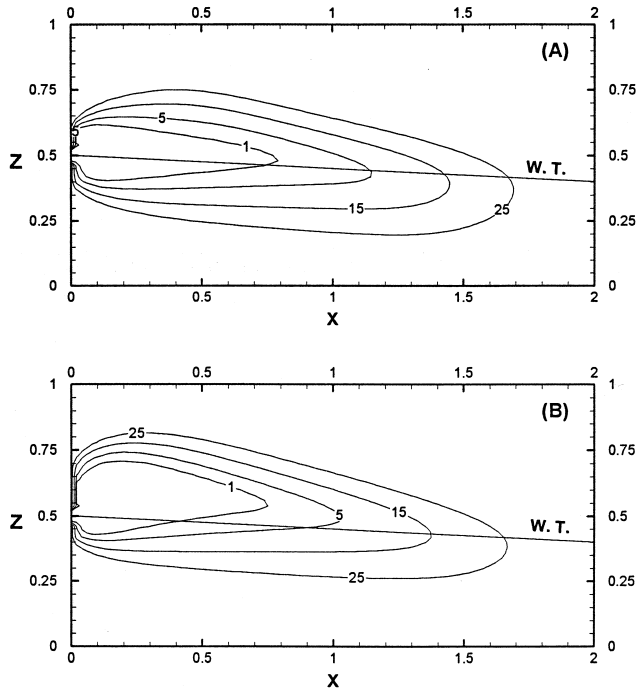


Fig. 6. Salinity contours (g/l) at $t = 100$ for Example 3. (A) The tracer case and (B) the density-dependent case. W.T. represents the water table. The initial salt concentration is 30 g/l.

zone. The term DD represents the density-dependent case and the term T represents the tracer case. The second criterion, criterion F , relates to the outflow from the domain:

$$F(\alpha, R) = \frac{\left(\frac{Q_u}{Q_s}\right)_{DD}}{\left(\frac{Q_u}{Q_s}\right)_T} \tag{15}$$

The terms Q_u and Q_s are the diluted masses outflowing from the domain above and below the water table, respectively. The criterion F was selected because for large R value, large amounts of diluted water left the domain by the end of the simulation.

The results are reported in Fig. 7a and b where both criteria show a decrease in the effects of buoyancy with an increasing α and/or an increasing R . The capillary fringe is small for large α values, hence, little water flow takes place in the unsaturated zone. Increasing R values causes the water flow to occur predominantly in the horizontal direction. In such a case, buoyancy effects are small because the vertical flow that results from buoyancy is small in comparison to the horizontal flow. The reader is referred to the work of Boufadel et al. (1999) for a thorough investigation of the contribution of capillary flow to total flow under steady-state conditions.

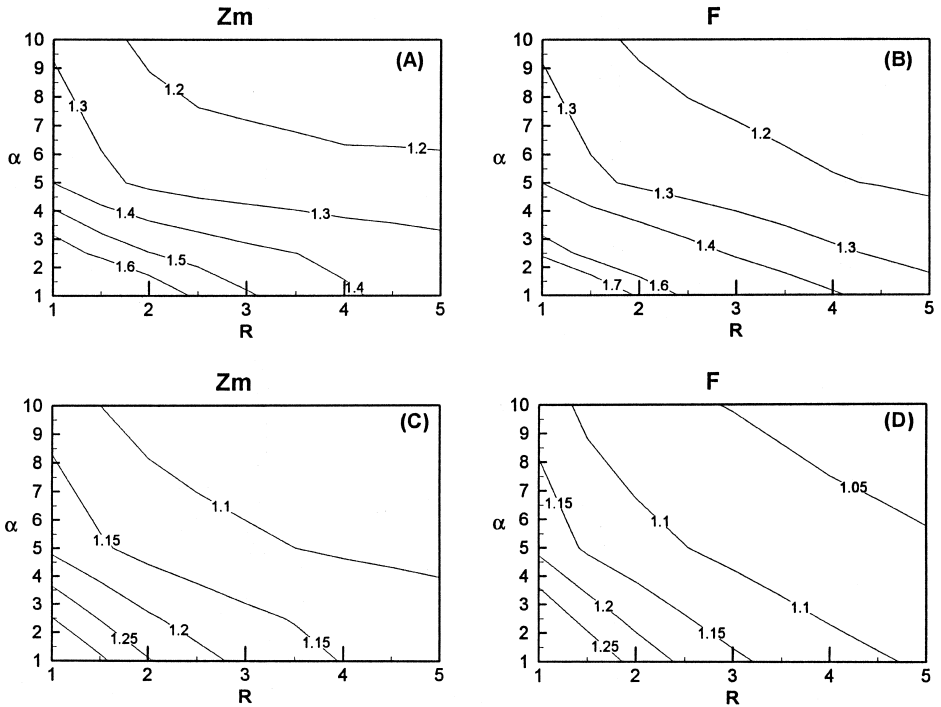


Fig. 7. Variation with α and R of the criteria Z_m and F at low dispersion (A) and (B), and at high dispersion (C) and (D). Higher values of Z_m or F imply increased buoyancy.

7.2. Effect of physical dispersion

Physical dispersion was shown by many researchers to cause a reduction in density gradients in isotropic saturated media (List, 1965; Schincariol et al., 1994; Fan and Kahawita, 1994; Schincariol et al., 1997). The effects of physical dispersion in variably saturated media are investigated here by doubling the dispersivity values to $a_L = a_T = 0.01$. These higher dispersivity values can be viewed to represent a sand with a wider grain size distribution than that used in Section 7.1 (Bear, 1972, p. 598; Ujfaludi, 1986).

The results are reported in Fig. 7c,d using the criteria Z_m and F , where less spreading of the freshwater in the unsaturated is deduced. Hence, similar to saturated media, the increase of physical dispersion in variably saturated media results in a decrease in the density gradients (or buoyancy).

The implications of the findings of this Section on bioremediation is that applying dissolved nutrients in a freshwater solution is advantageous only for beaches that are fine-textured, that have low isotropy ratios, and/or for beaches with a relatively narrow grain-size distribution.

The results given in Fig. 7 would probably overestimate the effect of buoyancy in a beach subjected to tidal action because it was observed by Forkel and Celia (1992) and by Boufadel et al. (1997) that density dependence in unsaturated media reaches its

maximum at a quasi steady state. A variable hydraulic boundary condition was not selected in this example because it would mask the physical phenomena that we seek to illustrate.

For the maximum salt concentrations considered in this example (30 g l^{-1}), results from partial coupling were indistinguishable from those of full coupling (until convergence within 1% of the dependent variables). Therefore, only the results of partial coupling were reported.

The simulation results of this Section were essentially unchanged when concentration-engendered viscosity effects were accounted for, which agrees with the finding of Section 6.1. The reader is referred to Welty and Gelhar (1992) for a thorough discussion of the effects of viscosity and density in various one-dimensional displacement scenarios.

The modeling approach used in this paper is general and can be used to study the movement of water-soluble hydrocarbons, such as methanol, in the subsurface. The example provided in this Section can be viewed as representing the breakage of a methanol pipe at the water table of an aquifer. The dimensionless nature of our approach allows for direct use of the numerical results provided proper scaling is conducted.

8. Summary and conclusions

A formulation for density-and-viscosity-dependent flow in two-dimensional variably saturated media was presented. The governing equations were cast in a dimensionless form that depends on six dimensionless parameters. The dimensionless form provides guidelines for scaling down natural system to the laboratory scale and a basis for comparing numerical results. The governing equations were discretized in the space using the Galerkin finite element formulation and integrated in time using backward Euler with mass lumping. The modified Picard method (Celia et al., 1990) was used to account for the nonlinearities when solving the equations in the unsaturated zone. The resulting numerical model, the MARUN model, was verified by comparison to published numerical results.

The MARUN model was used to investigate beach hydraulics at seawater concentration (30 g l^{-1}) in the context of nutrients delivery for bioremediation of oil spills on beaches. Numerical simulations in a rectangular section of a hypothetical beach revealed that buoyancy in the unsaturated zone is significant in soils that are fine textured, with low anisotropy ratio, and/or exhibiting small physical dispersion. In such situations, application of dissolved nutrients to a contaminated beach in a freshwater solution is superior to their application in a seawater solution.

The simulation results of this paper were essentially unchanged when concentration-engendered viscosity effects were accounted for. This observation agrees with the arguments of Galeati et al. (1992) and Schincariol et al. (1997) that in typical two-dimensional natural systems at concentrations close to seawater values (30 to 50 g l^{-1}), concentration-engendered viscosity effects are negligible with respect to concentration-engendered density effects.

Acknowledgements

This work was supported, in part, by the US Environmental Protection Agency's National Risk Management Research Laboratory, Cincinnati, OH under Cooperative Agreement No CR-821029. However, it does not necessarily reflect the views of the Agency, and no official endorsement should be inferred.

Appendix A

Eq. (6) is obtained by expanding the temporal derivative term in Eq. (3):

$$\frac{\partial(\beta\phi S)}{\partial t^*} = \beta\phi \frac{\partial S}{\partial t^*} + \beta S_o^* S \frac{\partial \psi^*}{\partial t^*} + \phi S \frac{\partial \beta}{\partial t^*} \quad (\text{A1})$$

The transport equation formulation given by (7) is more involved. The 'original' flow equation (i.e., prior to applying Darcy's law) is:

$$\frac{\partial(\rho^* \phi S)}{\partial t^*} = - \frac{\partial(\rho^* q_x^*)}{\partial x^*} - \frac{\partial(\rho^* q_z^*)}{\partial z^*}. \quad (\text{A2})$$

By dividing Eq. (A2) by ρ_o^* and rearranging, it results in:

$$\begin{aligned} \frac{\partial(\beta\phi S)}{\partial t^*} = \beta \frac{\partial(\phi S)}{\partial t^*} + \phi S \frac{\partial \beta}{\partial t^*} = - \beta \left[\frac{\partial q_x^*}{\partial x^*} + \frac{\partial q_z^*}{\partial z^*} \right] \\ + \left[-q_x^* \frac{\partial \beta}{\partial x^*} - q_z^* \frac{\partial \beta}{\partial z^*} \right] + Q. \end{aligned} \quad (\text{A3})$$

While the transport equation (5) is rewritten as:

$$\frac{\partial(\phi S c)}{\partial t^*} = c^* \frac{\partial(\phi S)}{\partial t^*} + \phi S \frac{\partial c^*}{\partial t^*} = \nabla(\phi S \underline{D}^* \nabla c^*) - \frac{\partial(q_x^* c^*)}{\partial x^*} - \frac{\partial(q_z^* c^*)}{\partial z^*}. \quad (\text{A4})$$

The right-hand side of Eq. (A4) is further developed to write:

$$\begin{aligned} c^* \frac{\partial(\phi S)}{\partial t^*} + \phi S \frac{\partial c^*}{\partial t^*} = \nabla(\phi S \underline{D}^* \nabla c^*) + c^* \left[- \frac{\partial q_x^*}{\partial x^*} - \frac{\partial q_z^*}{\partial z^*} \right] \\ + \left[-q_x^* \frac{\partial c^*}{\partial x^*} - q_z^* \frac{\partial c^*}{\partial z^*} \right]. \end{aligned} \quad (\text{A5})$$

After multiplying Eq. (A3) by c^* , dividing it by β , subtracting it from Eq. (A5), and taking into account the fact that $\delta\beta/\delta s = \epsilon^* \delta c^*/\delta s$ ($s = x^*, z^*, t^*$), Eq. (7) is obtained.

Models that use the volumetric formulation for the salt, assume that the spatial variation of the density is much smaller than the variation of the Darcy fluxes (Frind, 1982; Galeati et al., 1992; Fan and Kahawita, 1994; Xue et al., 1995), which is probably

due to the fact that these models are intended for seawater concentration only. This assumption is the equivalent of neglecting the second brackets in Eqs. (A3) and (A5), which results in a mass balance error. Although the mass balance error is small at low salt concentration, it can be very large at large salt concentration because high salinity gradients are usually associated with large salt concentrations (Hassanizadeh and Leijnse, 1988).

Appendix B. Notation

K_{x0} , K_{z0} , L_x , and L_z are dimensional quantities. The remaining terms are dimensionless except when they are starred.

a_L	Longitudinal dispersivity
a_T	Transverse dispersivity
c^*	Salt concentration
D	Dispersion tensor
\overline{D}_f	Diffusion coefficient
k_x	Horizontal permeability
k_z	Vertical permeability
K_x	Horizontal hydraulic conductivity
K_z	Vertical hydraulic conductivity
K_{x0}	Saturated horizontal hydraulic conductivity
K_{z0}	Saturated vertical hydraulic conductivity
L_x	Horizontal length of domain
L_z	Vertical length of domain
m, n	Parameters of the model of van Genuchten (1980)
q	The Darcy flux vector
q_x	Horizontal Darcy flux
q_z	Vertical Darcy flux
R	Ratio of anisotropy K_{x0}/K_{z0}
S	Saturation ratio
S_0	Elastic storage per unit fluid weight
S_e	Effective saturation ratio
S_r	Residual soil saturation
x	Horizontal coordinate
z	Vertical coordinate

Greek letters

α	A parameter of the model of van Genuchten (1980)
β	Ratio of saltwater density to freshwater density
δ	Fitting parameter for the viscosity–concentration curve
ϵ	Fitting parameter for the density–concentration curve
ϕ	Porosity
Ψ	Pressure head
τ	Tortuosity

References

- Anderson, D.A., Tannehill, J.C., Pletcher, R.H., 1984. Computational Fluid Mechanics and Heat Transfer. Mc. Hemisphere Publishing, p. 599.
- Bear, 1972, p. 598.
- Boufadel, M.C., 1998. Nutrient transport in beaches: effect of tides, waves, and buoyancy. PhD thesis, Department of Civil and Environmental Engineering, University of Cincinnati, Cincinnati, OH.
- Boufadel, M.C., Suidan, M.T., Venosa, D.A., 1997. Density-dependent flow in one-dimensional variably saturated media. *J. Hydrol.* 202, 280–301.
- Boufadel, M.C., Reeser, P., Suidan, M.T., Wrenn, B.A., Cheng, J., Du, X., Venosa, A.D., 1998a. Optimal nitrate concentration for the biodegradation of *n*-heptadecane in a variably saturated sand column. *Environmental Technology*, accepted.
- Boufadel, M.C., Suidan, M.T., Rauch, C.H., Venosa, A.D., Biswas, P., 1998b. 2-D variably-saturated flow: physical scaling and Bayesian estimation. *J. of Hydrologic Eng.* ASCE 3, 223–231.
- Boufadel, M.C., Suidan, M.T., Venosa, A.D., Bowers, M.T., 1999. Steady seepage from trenches and dams: contribution of capillary flow. *J. of Hydraulic Eng.* ASCE, in press.
- Celia, M.A., Bouloutas, E.T., Zarba, R.L., 1990. A general mass-conservative numerical solution for the unsaturated flow equation. *Wat. Resour. Res.* 26, 1483–1496.
- Cooley, R.L., 1983. Some new procedures for numerical solution of variably saturated flow problems. *Wat. Resour. Res.* 19, 1271–1285.
- CRC Handbook of Chemistry and Physics, 63rd edn, 1982–1983. Boca Raton, FL.
- Croucher, A.E., O'Sullivan, M.J., 1995. The Henry problem for saltwater intrusion. *Wat. Resour. Res.* 31, 1809–1814.
- Elder, J.W., 1967. Transient convection in a porous medium. *J. Fluid Mech.* 27, 609–623.
- Fan, Y., Kahawita, R., 1994. A numerical study of variable density flow and mixing in porous media. *Wat. Resour. Res.* 30, 2707–2716.
- Forkel, C., Celia, M.A., 1992. Numerical simulation of unsaturated flow and contaminant transport with density and viscosity dependence. *Computational Methods in Water Resources IX, Vol. 2. Mathematical Modeling in Water Resources. Computational Mechanics Publications, MA*, pp. 351–359.
- Freeze, R.A. Cherry, J.A., 1979. *Groundwater*. Prentice-Hall, Englewood Cliffs, NJ, p. 604.
- Frind, E.O., 1982. Simulation of long-term transient density-dependent transport in groundwater. *Adv. Wat. Resour.* 5, 73–88.
- Galeati, G., Gambolati, G., Neuman, S.P., 1992. Coupled and partially coupled Eulerian–Lagrangian model of freshwater–seawater mixing. *Wat. Resour. Res.* 28, 149–165.
- Gundlach, E.R., 1987. Oil-holding capacities and removal coefficients for different shoreline types to computer simulate spills in coastal waters. *Proc. 1987 Int. Oil Spill Con. American Petroleum Institute, Washington, DC*, pp. 451–457.
- Gureghian, A.B., 1983. TRIPM: a two-dimensional finite-element model for the simultaneous transport of water and reacting solutes through saturated and unsaturated porous media. Technical Report, Battelle Memorial Institute, Columbus.
- Hassanizadeh, S.M., Leijnse, T., 1988. On the modeling of brine transport in porous media. *Wat. Resour. Res.* 24, 321–330.
- Hayes, M.O., 1972. Forms of sediment accumulation in the beach zone. In: Meyer, R.E. (Ed.), *Waves on Beaches and Resulting Sediment Transport*. Academic Press, New York, pp. 297–356.
- Henry, H.R., 1964. Effects of dispersion on salt encroachment in coastal aquifers. *U.S. Geol. Surv. Water Supply Paper 1613-C*, pp. C71–C84.
- Herbert, A.W., Jackson, C.P., Lever, D.A., 1988. Coupled groundwater flow and solute transport with fluid density strongly dependent on concentration. *Wat. Resour. Res.* 24, 1781–1795.
- Huyakorn, P.S., Pinder, G.F., 1983. *Computational Methods in Subsurface Flow*. Academic Press, New York, p. 473.
- Huyakorn, P.S., Mercer, J.W., Ward, D.S., 1985. Finite element matrix and mass balance computational schemes for transport in variably saturated porous media. *Wat. Resour. Res.* 21, 346–358.
- Huyakorn, P.S., Mercer, J.W., Ward, D.S., 1987. Saltwater intrusion in aquifers: development and testing of a three-dimensional finite element model. *Wat. Resour. Res.* 23, 293–312.

- Istok, J., 1989. Groundwater modelling by the finite element method. American Geophysical Union, Washington.
- List, E.J., 1965. The stability and mixing of a density-stratified horizontal flow in a saturated porous medium. Rep. KH-R-11, Calif. Inst. of Tech., Pasadena.
- Najem, W., 1982. Introduction Aux Techniques du Calcul Numerique (in French), 2nd edn. Saint Joseph University, Lebanon, p. 54.
- Oldenburg, C.M., Pruess, K., 1995. Dispersive transport dynamics in a strongly coupled groundwater–brine flow system. *Wat. Resour. Res.* 31, 289–302.
- Pinder, G.F., Gray, W.G., 1977. Finite Element Simulation in Surface and Subsurface Hydrology. Academic Press, New York, p. 294.
- Ronen, D., Yechieli, Y., Shatkey, M., 1996. Characterization of water and solute transport in the unsaturated zone of a hypersaline environment. *Wat. Resour. Res.* 32 (11), 3267–3327.
- Schincariol, R.A., Schwartz, F.W., Mendoza, C.A., 1994. On the generation of instabilities in variable density flow. *Wat. Resour. Res.* 30, 913–927.
- Schincariol, R.A., Schwartz, F.W., Mendoza, C.A., 1997. Instability in variable density flows: stability and sensitivity analyses for homogeneous and heterogeneous media. *Wat. Resour. Res.* 33, 31–41.
- Ujfaludi, L., 1986. Longitudinal dispersion tests in non-uniform porous media. *Hydrol. Sci.* 31, 4.
- Usseglio-Polatera, J.M., Aboujaoude, A., Molinaro, P., Rangogni, R., 1990. 3-D Modeling of coupled groundwater flow and transport within saturated and unsaturated zones. In: Gambolati, G., Rinaldo, A., Brebbia, C.A., Gray, G.W., Pinder, G.F. (Eds.), *Computational Methods in Subsurface Hydrology*. Proceedings of the 8th International Conference on Computational Methods in Water Resources, Venice, Italy.
- van Genuchten, M.Th., 1980. A closed-form equation for predicting the hydraulic conductivity of unsaturated soils. *Soil Sci. Soc. Am. J.* 44, 892–898.
- Venosa, A.D., Suidan, M.T., Wrenn, B.A., Strohmeier, K.L., Haines, J.R., Eberhart, B.L., King, D., Holder, E., 1996. Bioremediation of an experimental oil spill on the shoreline of Delaware Bay. *Environ. Sci. Technol.* 30, 1764–1775.
- Voss, C.I., Souza, W.R., 1987. Variable density flow and solute transport simulations of regional aquifers containing a narrow freshwater–saltwater transition zone. *Wat. Resour. Res.* 23 (10), 1851–1866.
- Waddell, E., 1976. Swash–groundwater–beach profile interactions. *Spec. Publ.* 24, Society of Economic Paleontologists and Mineralogists, pp. 115–125.
- Welty, C., Gelhar, L.W., 1992. Simulation of large-scale transport of variable density and viscosity fluids using a stochastic mean model. *Wat. Resour. Res.* 28, 815–827.
- Wise, W.B., Guven, O., Molz, F.J., McCutcheon, S.C., 1994. Nutrient retention time in high-permeability, oil-fouled beach. *ASCE J. Environ. Eng.* 120, 1361–1379.
- Wooding, R.A., Tyler, S.W., White, I., 1997a. Convection in groundwater below an evaporating salt lake: 1. Onset of instability. *Wat. Resour. Res.* 33, 1199–1217.
- Wooding, R.A., Tyler, S.W., White, I., Anderson, P.A., 1997b. Convection in groundwater below an evaporating salt lake: 2. Evolution of fingers or plumes. *Wat. Resour. Res.* 33, 1219–1228.
- Wrenn, A.B., Suidan, M.T., Strohmeier, K.L., Eberhart, B.L., Wilson, G.J., Venosa, A.D., 1997. Nutrient transport during oil-spill bioremediation: evaluation with lithium as a conservative tracer. *Wat. Res.* 31, 515–524.
- Xue, X., Xie, C., Wu, J., 1995. A three-dimensional miscible transport model for seawater intrusion in China. *Wat. Resour. Res.* 31, 903–912.
- Yeh, G.T., 1981. On the computation of the Darcian velocity and mass balance in the finite element modeling of groundwater flow. *Wat. Resour. Res.* 17, 1529–1534.
- Yeh, G.T., Ward, D.S., 1981. FEMWASTE: a finite-element model of waste transport through saturated–unsaturated porous media. Rep. ORNL-5601, Oak Ridge Natl. Lab., Oak Ridge, TN, p. 137.